Structure and magnetism of Fe thin films grown on Rh(001) studied by photoelectron spectroscopy

K. Hayashi,[1] M. Sawada,[1] A. Harasawa,[1] A. Kimura,[2] and A. Kakizaki[1,3,*]

[1]*Institute for Solid State Physics, University of Tokyo, Chiba 277-8581, Japan*
[2]*Department of Physical Sciences, Hiroshima University, Hiroshima 739-8526, Japan*
[3]*Institute of Materials Structure Science, High Energy Accelerator Research Organization, Ibaraki 305-0801, Japan*

Structural and magnetic properties of Fe thin films grown epitaxially on Rh(001) are studied by spin- and angle-resolved valence-band photoemission, Fe $2p_{3/2}$ photoelectron diffraction, and x-ray magnetic circular dichroism experiments. The valence-band structure shows characteristic features of a fcc high-spin state at 4 monolayers (ML) and those of ferromagnetic bulk bcc Fe at 8 ML. The structure of the Fe film reveals fct(001) compressed along the direction perpendicular to the surface in the low-coverage region and gradually changes to distorted bcc(110) as the film thickness increases. The magnetic moments increase as a function of the film thickness and reach the same value as in bulk bcc Fe above 6 ML. The Fe films show in-plane ferromagnetism above 2 ML, and the thickness dependence of the magnetic properties is discussed in connection with the characteristic growth mode.

I. INTRODUCTION

Magnetism of solid surfaces and thin films has been a rapidly growing research field in recent decades. One of the main reasons is that their lower symmetry and smaller coordination number are expected to show different aspects of magnetic properties of materials from those of the bulk. Thin films of magnetic materials have been investigated in particular to clarify the transition from two- to three-dimensional magnetic behavior, where the evolution of electronic states causing ferromagnetism with increasing film thickness is of particular interest. As characteristic example of $3d$ transition metal ferromagnets, extensive studies on the structures and magnetic properties of Fe films have been made theoretically[1–6] and experimentally[7–22] to contribute to the microscopic description of ferromagnetism.

Bulk Fe is known to be a bcc structure at room temperature (RT) and ferromagnetic below 920 K. On the other hand, Fe films grown on nonmagnetic substrates show a variety of structures and magnetism depending on the size of the lattice-constant (a_0) difference between the substrate and bulk bcc Fe ($a_0 = 2.87$ Å). On Au(001) ($a_0 = 4.07$ Å),[8] and Ag(001) ($a_0 = 4.08$ Å),[9,10] Fe films grow in a bcc structure and are ferromagnetic due to a small lattice mismatch with the Fe(001) surface ($\sqrt{2}a_0 = 4.05$ Å). On Cu(001) ($a_0 = 3.58$ Å),[11–16] and Co(001) ($a_0 = 3.54$ Å),[17,18] Fe films start to grow layer by layer in a face-centered tetragonal (fct) structure with a lattice distance elongated along the direction perpendicular to the surface, and show ferromagnetism below 5 monolayers (ML). In the 6–10 ML region, they show fcc structure, which is achieved at high temperature in bulk Fe, and only the topmost few layers are found to be ferromagnetic.[13] As the thickness increases over 11 ML, the Fe film changes its structure as a whole to a bcc structure with the (110) plane parallel to the substrate surface. This is explained by the stability of the crystal structure under a strong strain field. The origin of this complicated structural and magnetic behavior has been investigated theoretically by a first-principles calculation of the total energy and magnetic moments.[4] Recently, Schmitz *et al.*[19] obtained the thickness

dependence of the Fe $3d$ spin (m_{spin}) and orbital (m_{orb}) magnetic moments by magnetic circular dichroism (MCD) in an x-ray absorption spectroscopy experiment. They showed that Fe films grown on Cu(001) and Co(001) substrates reveal three different magnetic behaviors depending on the thickness. Up to 4 ML, the Fe film is ferromagnetic as a whole. Between 5 and 10 ML Fe, the average m_{spin} is diminished, which suggests that only the surface region of the film is ferromagnetically ordered. Over 11 ML, the Fe films are homogeneously ferromagnetic. Schmitz *et al.* suggested the importance of the structural and electronic properties at the interface. However, the relationship between the structure and magnetic properties of Fe films is not yet fully understood.

In this article, we discuss the structural and magnetic properties of Fe films epitaxially grown on a Rh(001) ($a_0 = 3.80$ Å) surface. The atomic distance of Rh(001) has an intermediate value between Cu(001) and Au(001), and the structure and magnetism of Fe films on Rh(001) are still controversial. Fe films grown at 350 K were reported to be in a fct structure at the initial growth stage,[20] while a quantitative low-energy electron diffraction study of films grown at RT showed a bcc structure below 5 ML.[21] The magnetic properties of Fe films on Rh(001) were investigated by spin-polarized neutron reflection, and it was shown that the Fe film does not show in-plane ferromagnetism.[22] In the following, we present angle-resolved photoemission (ARPES) and spin- and angle-resolved photoemission (SARPES) spectra to study the valence-band structure of Fe films and its thickness dependence. We also present Fe $2p_{3/2}$ x-ray photoelectron diffraction (XPD) and MCD spectra measured at the Fe $2p$ and Rh $3p$ absorption edges to investigate the structure and magnetism of Fe films.

II. EXPERIMENT

ARPES and Fe $2p_{3/2}$ XPD experiments were carried out at beamline 18A of the Photon Factory using a standard ARPES system with a sample preparation apparatus in which a reflection high-energy electron diffraction (RHEED) system was installed for the present study. ARPES spectra
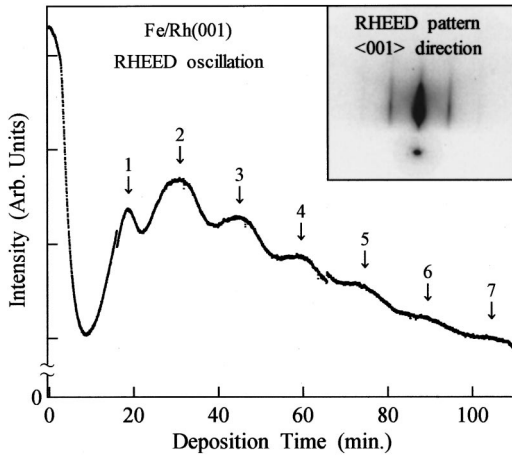
FIG. 1. Intensity of specular beam spot of RHEED pattern (inset) as a function of the deposition time.

were measured in the normal-emission mode using synchrotron radiation with varying incident photon energy. The polarization vector of incoming light was chosen to be parallel to two different mirror planes, i.e., Rh(010) and Rh(110), to facilitate the analysis of the symmetry of the electronic states obtained from the ARPES spectra. The Fe $2p_{3/2}$ XPD patterns were observed using a Mg $K\alpha$ (1253.6 eV) x-ray source and rotating the analyzer around the sample in the mirror planes with an angular step of 1°. The angle resolution was 0.5°. The SARPES spectra were measured using a He discharge lamp and a SARPES spectrometer consisting of a hemispherical electron energy analyzer and a compact retarding-type Mott detector.[23] The MCD experiments were carried out at beamline 11A using right- and left-circularly polarized synchrotron radiation from a dipole magnet. The x-ray absorption spectra were measured by the photocurrent at the Fe $2p$ and Rh $3p$ absorption edges. The sample was magnetized along the $\langle 110 \rangle$ axes parallel to the surface and at 30° with respect to the direction of the incident photons.

The Rh(001) surface was cleaned *in situ* by repeated cycles of Ar ion bombardment for several hours followed by annealing at 1350 K for 5 min. The clean Rh(001) surface was confirmed by observing C $1s$ and O $1s$ XPS spectral intensities to be below the detection limit. Clear 1×1 RHEED patterns confirmed the flatness of the Rh(001) surface. Fe films were prepared by deposition using an evaporation source after an extensive degassing of the source. The pressure during the evaporation was kept below 2×10^{-10} mbar and a typical deposition rate was 0.2 ML/min. The temperature of the Rh(001) substrate was kept at 350 K and RT for the sake of comparison with previous work.[20,21] The base pressure of the measuring system was below 1×10^{-10} mbar.

III. RESULTS AND DISCUSSION

Figure 1 shows the intensity of the specular beam spot of the RHEED patterns as a function of the deposition time, which evidenced an epitaxial and layer-by-layer growth of the Fe films. We observed no change in 1×1 RHEED patterns during film growth below 12 ML. This indicates that

the intra-atomic spacing of the deposited Fe film was the same as that of the Rh(001) substrate. We estimated that the in-plane lattice constant of the Fe film is 3.80 ± 0.15 Å.

To investigate the thickness dependence of the electronic structure of Fe films, we measured ARPES spectra with photon energies from 12 to 76 eV. The angle of incident light was 45° off normal and photoelectrons emitted normal to the surface were collected. Figure 2(a) shows the valence-band spectra of a 4 ML film grown at 350 K. We derived the experimental energy band structure by assuming a free-electron final state for the photoelectrons and an inner potential of 10 eV. The results are shown in a color scale in Fig. 2(b) together with a theoretical band calculation along the Γ-X direction of the Brillouin zone (BZ) for fcc Fe in the high-spin state.[24,25] The experimentally obtained valence bands satisfactorily reproduce the $\Delta_{1\uparrow}$ and $\Delta_{5\uparrow}$ bands with energy dispersion between 0 and 2 eV. The peaks near the Fermi level observed in the ARPES spectra correspond to the $\Delta_{1\downarrow}$ and $\Delta_{5\downarrow}$ bands. The bands with large energy dispersion between 5 and 8 eV are assigned as $\Delta_{1\uparrow}$ and $\Delta_{1\downarrow}$ bands, respectively. In Fig. 2(a), comparatively weak spectral features appear at the binding energies of 3.5 and 5 eV in the spectra with excitation energies above 44 eV. They possibly originate from bands with a large density of states at the X point in the neighboring BZ and are observed due to rather poor momentum resolution in the ARPES spectra excited with high photon energies.[26] This assignment of the valence bands was confirmed by the polarization dependence of the ARPES spectra observed with two different angles of incident light, 30° and 75° off normal. We found that the dispersion of the Δ_5 bands was more evident in the spectra observed at 30° off normal than at 75°. This is consistent with the theoretically expected polarization dependence of the ARPES spectra in normal-emission mode.[27] The agreement between the experimental results and the theoretical band calculation implies that the Fe film in the low-coverage region resembles high-spin fcc Fe.

Figure 3(a) shows the ARPES spectra of the Fe film at high coverage (8 ML). The experimental configuration was the same as that of the 4 ML film. The observed spectral profiles and their photon energy dependence are quite different from Fig. 2(a). The peaks observed near the Fermi level and assigned to be $\Delta_{5\uparrow}$ bands in the spectra of the 4 ML film do not appear in those of the 8 ML film. Instead, we observe peaks at 0.5, 2, and 3 eV with small energy dispersion. The experimentally obtained band structure shown in Fig. 3(b) shows considerable deviation from the calculated one for fcc Fe. In the figure, we present the calculated band structure along the Γ-N direction of the BZ for bcc Fe.[25,28] The agreement between experimentally obtained band structure and calculation is rather good. The bands near the Fermi level observed with excitation energies below 40 eV correspond to $\Sigma_{1\uparrow,\downarrow}$ and $\Sigma_{4\uparrow}$ bands. The observed bands with small energy dispersion at binding energies around 2 and 3 eV correspond to $\Sigma_{1\uparrow}$ band. The weak spectral features appeared at the binding energy of 5.5 eV in the spectra with excitation energies above 44 eV are observed for the same reason as in the case of the 4 ML film. They originate from the large density
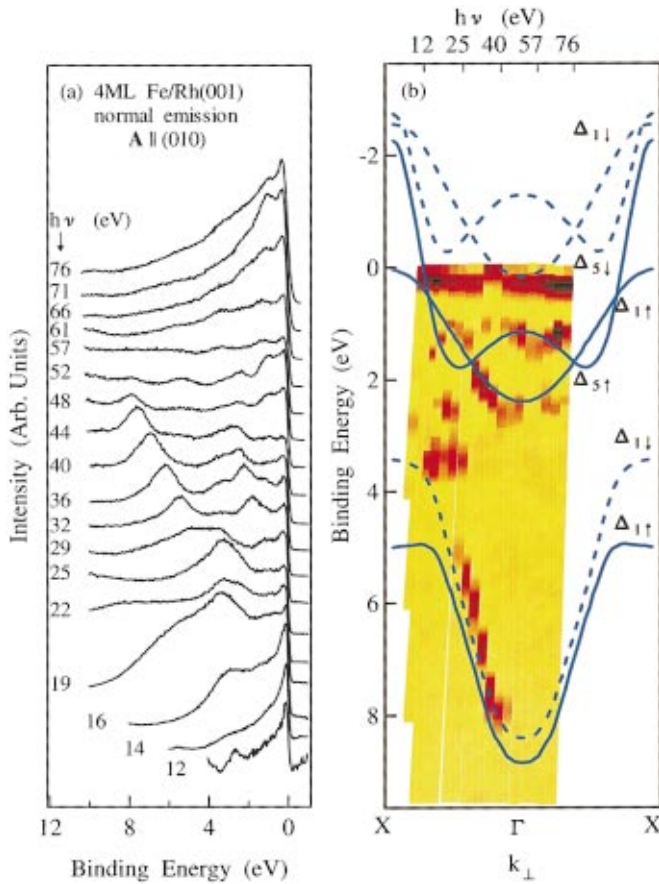
FIG. 2. (Color) (a) ARPES spectra of 4 ML Fe film grown at 350 K. (b) Experimentally obtained valence-band structure (second derivative image of EDC) is presented by a color scale. Calculated valence bands along the Γ-X direction of fcc BZ are presented by solid and dotted lines.

FIG. 3. (Color) (a) ARPES spectra of 8 ML Fe film grown at 350 K. (b) Experimentally obtained valence-band structure (second derivative image of EDC) is presented by a color scale. Calculated valence bands along the Γ-N direction of bcc BZ are presented by solid and dotted lines.

of states near the N point in the neighboring BZ. We also measured the polarization dependence of the spectra and confirmed that the band near the Fermi level originates from the $\Sigma_{4\uparrow}$ band.

To study the relationship between electronic structure and magnetism of the Fe films, we also measured SARPES spectra of 4 and 8 ML films in the normal-emission mode. The observed majority- and minority-spin spectra at the two film thicknesses show quite different spectral profiles in Fig. 4. Since we used unpolarized light, the SARPES spectra of both film thicknesses consist of more features than observed in Figs. 2(a) and 3(a). For the 4 ML film the majority-spin spectrum clearly shows peak features corresponding to $\Delta_{1\uparrow}$ and $\Delta_{5\uparrow}$ bands in the middle point of the BZ, while in the minority-spin spectrum the peak corresponding to the $\Delta_{1\downarrow}$ band is also obvious. The SARPES spectra of the 8 ML film show three spectral features in the majority-spin spectrum, which originate from the $\Sigma_{1\uparrow}$ and $\Sigma_{4\uparrow}$ bands. The prominent peak observed close to the Fermi level in the minority-spin spectrum corresponds to the $\Sigma_{1\downarrow}$ band. It is evident that the 4 and 8 ML films reveal the spin-dependent electronic structures of the fcc and bcc phases, respectively. In polarized neutron scattering experiments, Bland, Pescia, and Willis[22] did not observe in-plane ferromagnetism. We have measured

the SARPES spectra with applied magnetic field in the $\langle 110 \rangle$ direction parallel to the surface. Our results clearly show that both 4 and 8 ML films are magnetized along the $\langle 110 \rangle$ easy magnetization direction and demonstrate exchange-split valence bands in the BZ perpendicular to the surface.

From the results of ARPES and SARPES, we conclude that the electronic structure and magnetic properties of Fe films epitaxially grown on Rh(001) change depending on the film thickness; this may originate from the thickness dependence of the geometric structure of the Fe films. Since the 1×1 RHEED patterns do not show any thickness dependence below 12 ML, the interlayer spacing of the Fe film would cause the change of the structure of the films from fcc(001) at low coverage to bcc(110) at high coverage. To investigate the growth mode of Fe films, we measured the angular distribution of Fe $2p_{3/2}$ core-level photoelectron intensity, i.e., XPD patterns, for various film thicknesses. The photoelectrons with kinetic energies above a few hundred eV exhibit a pronounced enhancement in their intensities along the axes toward neighboring atoms due to the constructive interference between the directly emitted and scattered outgoing waves. The angular distribution of photoelectrons provides information on the spatial distribution of atoms near the surface.[29]
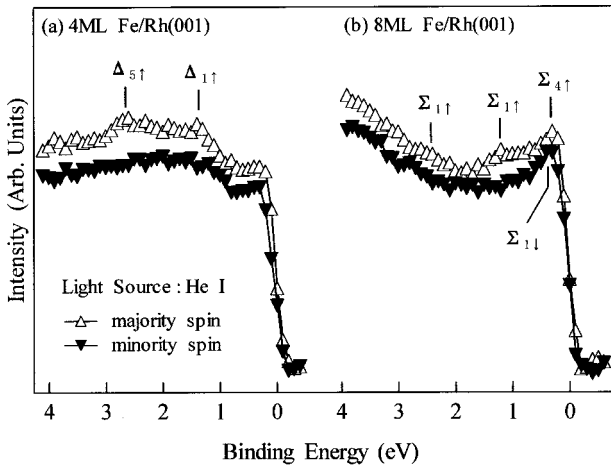
FIG. 4. Spin-resolved photoemission spectra of (a) 4 and (b) 8 ML Fe films. Upward and downward triangles show majority- and minority-spin spectra, respectively.

Figure 5(a) shows the Fe $2p_{3/2}$ XPD patterns observed in the (010) plane of the Rh(001) substrate. In the figure, each pattern consists of a few peaks. For Fe films with thickness over 3 ML, the peaks are observed at $\theta = 0°$ and near 50°, which correspond to interference of the forward scattering waves along the $\langle 001 \rangle$ and $\langle 101 \rangle$ directions, respectively. The
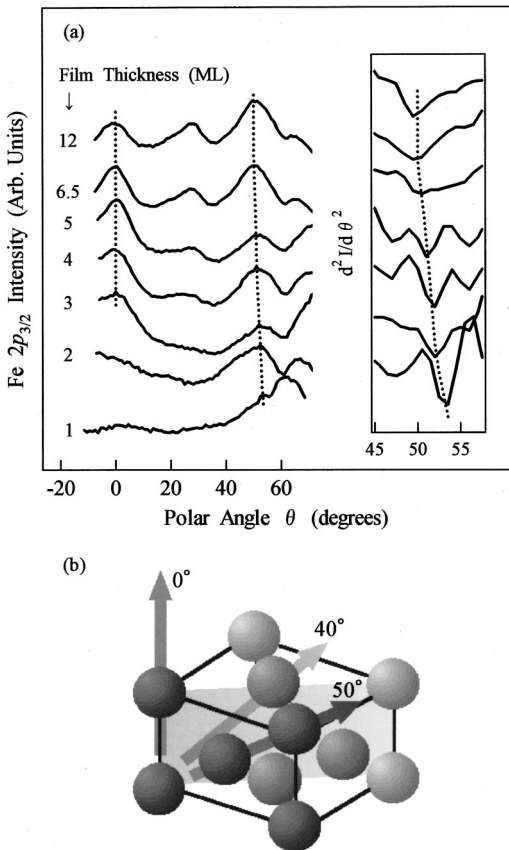
FIG. 5. (a) Fe $2p_{3/2}$ XPD patterns observed in Rh(010) plane for various Fe film thicknesses. (b) Schematics of the crystallographic structure of Fe film.
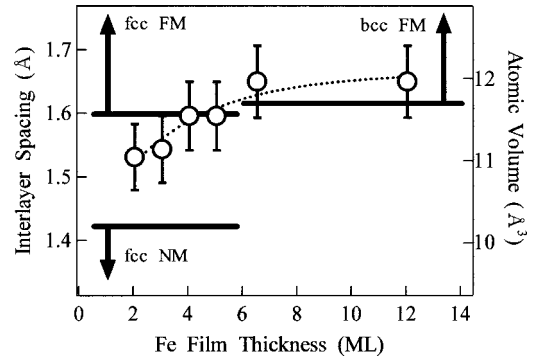
FIG. 6. Interlayer spacing for various Fe film thicknesses obtained from XPD measurements. The right ordinate scales the atomic volume of Fe. Bold lines represent the theoretically obtained threshold of atomic volumes for ferromagnetic fcc and bcc Fe and nonmagnetic fcc Fe.

peaks observed around 30°, which appear in the patterns of the films over 4 ML, correspond to interference along the direction $\langle 103 \rangle$. It should be noted in the figure that the peak around 50° tends to shift its position toward smaller angles as the film thickness increases, which corresponds to increase of the interlayer spacing of the Fe film. By obtaining the second derivative of the XPD intensity, we found that the amount of shift is 2.5° as the thickness increases up to 6 ML. We did not observe a peak shift over 6 ML. The thickness dependence of the peak position was also observed at 30°, although less evident than the peak shift at 50°. To confirm the peak shift in XPD patterns, i.e., the increase of the interlayer spacing with increase of the Fe film thickness, we also measured XPD patterns in the Rh(110) plane. We observed the shift of the peak appearing at 40°, which corresponds to interference along the $\langle 112 \rangle$ direction of the fcc lattice [Fig. 5(b)], to be 1.7° as the thickness increases up to 6 ML. The value obtained is consistent with an increase of the interlayer spacing of Fe films observed in the Rh(010) plane. Recently, Hwang, Swan, and Hong[30] also suggested that Fe films might grow in the tetragonally distorted cubic structure on Rh(001). Previously, Egawa *et al.*[20] observed the angular distribution of Fe *LMM* Auger electrons to investigate the structure of Fe films grown on a Rh(001) surface. However, they did not observe a thickness dependence of the peak position and reached the conclusion that Fe films reveal a fcc structure in a wide range of film thickness. This is probably due to less angular resolution ($\Delta \theta = 5°$) than the peak shift observed in the present work.

We evaluated the interlayer spacing of Fe films to be 1.53 ± 0.05 Å in the initial growth stage and plotted the result in Fig. 6. The interlayer spacing increases with increasing film thickness and reaches a constant value of 1.66 ± 0.06 Å at 6 ML. The figure shows that on Rh(001) Fe films start to grow in a compressed structure along the direction perpendicular to the surface and the degree of compression is released as the film thickness increases. The interlayer spacing changes continuously with film thickness and there is no evidence of a structural change as a whole as in the case of Fe films on Cu(001) and Co(001) surfaces.[13,18] In the Fe/Cu(001) and Fe/Co(001) systems, Fe films thicker than 11

ML cannot hold the structure elongated perpendicular to the surface and form edge dislocations at the interface to adjust lattice mismatch and reduce the total energy. In Fe films grown on Rh(001), the lattice mismatch is adjusted by the strain at the interface and the Fe film tends to gradually change from fct(001) to a distorted bcc(110) structure without a structural change as a whole. Since the surface sensitivity of the present photoelectron spectroscopy is less than 10 Å, the observed structural change occurs in the surface region of the Fe film. The fct(001) structure near the interface can hold regardless of Fe film thickness.

According to first-principles calculation of the total energy and magnetic moment of Fe films, the stability of ferromagnetism strongly depends on the lattice constant, in other words, the atomic volume of Fe.[21,31] The ferromagnetic phase is stable when the average atomic volume (v) exceeds a certain value. It has been predicted that ferromagnetism is stable in fcc Fe for $v > 11.57 \text{ Å}^3$, and in bcc Fe for $v > 11.7 \text{ Å}^3$. Based on the RHEED and XPD observations, we evaluated the atomic volume of Fe for each film thickness; this is shown on the right ordinate in Fig. 6. In the figure, Fe films realize ferromagnetism in the fcc structure at thickness over 4 ML and bcc ferromagnetism over 6 ML. The atomic volume of Fe in the current study exceeds the threshold of the nonmagnetic phase.

To investigate the thickness dependence of the magnetic properties we studied MCD, since the intensity of MCD spectra is directly related to the local magnetic moment of atoms in the film. We measured MCD spectra near Fe $2p$ and Rh $3p$ absorption edges for various film thicknesses. Figure 7(a) shows the Fe $2p_{3/2}$ MCD intensities normalized to the edge jump, which increase as a function of film thickness and reach a constant value of about 150% at 6 ML. We did not observe MCD for the Fe films below 2 ML, which is consistent with the results of the atomic volume consideration in Fig. 6. Nor did we observe MCD at the Rh $3p$ absorption edge regardless of the Fe film thickness. This implies that there is no induced magnetic moment in Rh atoms at the interface in spite of the possible existence of hybridization between Fe $3d$ and Rh $4d$ states. In the Fe/Rh(001) system it is considered that the first and second layers are nonmagnetic while only the upper layers are ferromagnetic in Fe films thicker than 2 ML. The interlayer spacing near the interface does not change with film thickness and is shorter that that of upper layers. Since the XPD results in Fig. 6 shows that the interlayer spacing increases toward the surface, the topmost few layers from the surface change their structures from fct(001) to distorted bcc(110) as the film thickness increases.

By applying the sum rule for MCD,[32] we evaluated m_{spin} and the ratio of m_{orb} to m_{spin} of Fe atoms in the film. The results are shown in Fig. 7(a). The expectation value of the magnetic dipole operator was neglected. In Fig. 7(a), m_{spin}
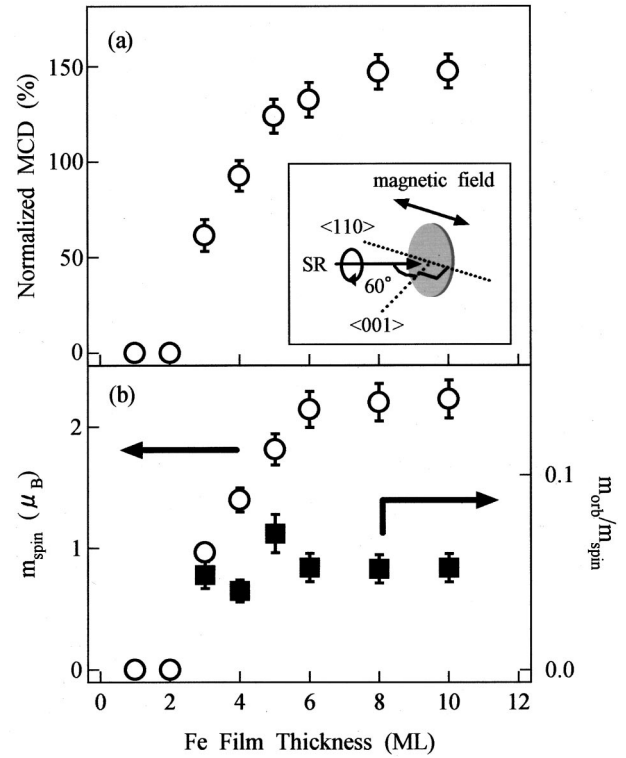
FIG. 7. (a) Thickness dependence of Fe $2p_{3/2}$ MCD intensity measured at RT. Inset is the geometry of MCD experiments. (b) Spin magnetic moment (m_{spin}) and the ratio of orbital magnetic moment (m_{orb}) to m_{spin} obtained from MCD sum rule.

shows similar thickness dependence to the MCD intensity and reaches $(2.14 \pm 0.21)\mu_B$ at 6 ML. It is almost the same value as in bulk bcc Fe,[33] and it is reasonable to suppose that Fe films become bcc above 6 ML. The m_{spin} and MCD intensity originate from the local magnetic moment of Fe in the film and follow the temperature dependence of the macroscopic magnetization which vanishes above the ferromagnetic transition temperature (T_c). The thickness dependence shown in Figs. 7(a) and 7(b) implies that the Fe film considerably reduces its T_c with decreasing film thickness which results in the small local magnetic moment observed at RT. The reduction of T_c due to the lower symmetry was also observed in Fe films grown on Au(001) and Ag(001) surfaces.[8,9] It is also observed that the ratio $m_{\text{orb}}/m_{\text{spin}}$ seems independent of the film thickness. This ratio is expected to increase with decreasing film thickness because of the reduced crystal field for thin films. For further investigation, MCD experiments at low temperature are needed in the future.

---

*Author to whom correspondence should be addressed.

[1] D. Bagayoko and J. Callaway, Phys. Rev. B **28**, 5419 (1983).

[2] C. L. Fu and A. J. Freeman, Phys. Rev. B **35**, 925 (1987).

[3] V. L. Moruzzi, P. M. Marcus, and P. C. Pattnaik, Phys. Rev. B **37**, 8003 (1988).

[4] V. L. Moruzzi, P. M. Marcus, and J. Kübler, Phys. Rev. B **39**, 6957 (1989).

[5] G. W. Fernando and B. R. Cooper, Phys. Rev. B **38**, 3016 (1988).

[6] T. Asada and S. Blügel, Phys. Rev. Lett. **79**, 507 (1997).

[7] S. D. Bader and E. R. Moog, J. Appl. Phys. **61**, 3729 (1987).

[8] W. Dürr, M. Taborelli, O. Paul, R. Germar, W. Gudat, D. Pescia, and M. Landolt, Phys. Rev. Lett. **62**, 206 (1989).

[9] B. T. Jonker, K.-H. Walker, E. Kisker, G. A. Prinz, and C. Carbone, Phys. Rev. Lett. **57**, 142 (1986).

[10] M. Stampanoni, A. Vaterlaus, M. Aeschlimann, and F. Meier, Phys. Rev. Lett. **59**, 2483 (1987).

[11] D. P. Pappas, K.-P. Kämper, B. P. Miller, H. Hopster, D. E. Fowler, A. C. Luntz, C. R. Brundle, and Z.-X. Shen, J. Appl. Phys. **69**, 5209 (1991).

[12] J. Giergiel, J. Shen, J. Woltersdorf, A. Kirilyuk, and J. Kirschner, Phys. Rev. B **52**, 8528 (1995).

[13] J. Thomassen, F. May, B. Feldmann, M. Wuttig, and H. Ibach, Phys. Rev. Lett. **69**, 3831 (1992).

[14] P. Xhonneux and E. Courtens, Phys. Rev. B **46**, 556 (1992).

[15] P. Schmailzl, K. Schmidt, P. Bayer, R. Döll, and K. Heintz, Surf. Sci. **312**, 73 (1994).

[16] B. Gubanka, M. Donath, and F. Passek, J. Magn. Magn. Mater. **161**, L11 (1996).

[17] E.-J. Escorcia-Aparicio, R. K. Kawakami, and Z. Q. Qui, Phys. Rev. B **54**, 4155 (1996).

[18] R. Kläsges, D. Schmitz, C. Carbone, W. Eberhardt, and T. Kachel, Solid State Commun. **107**, 13 (1998).

[19] D. Schmitz, C. Charton, A. Scholl, C. Carbone, and W. Eberhardt, Phys. Rev. B **59**, 4327 (1999).

[20] C. Egawa, Y. Tezuka, S. Oki, and Y. Murata, Surf. Sci. **283**, 338 (1993).

[21] A. M. Begley, S. K. Kim, F. Jona, and P. M. Marcus, Phys. Rev. B **48**, 1786 (1993).

[22] J. A. C. Bland, D. Pescia, and R. F. Willis, Phys. Rev. Lett. **58**, 1244 (1987).

[23] S. Qiao, A. Kimura, A. Harasawa, M. Sawada, J.-G. Chung, and A. Kakizaki, Rev. Sci. Instrum. **68**, 4390 (1997).

[24] M. Podgórny, J. Magn. Magn. Mater. **78**, 352 (1989).

[25] The theoretical band structure is plotted on the scale of momentum evaluated from the interlayer spacing in Fig. 6.

[26] A. A. Hezaveh, G. Jennings, D. Pescia, R. F. Willis, K. Prince, M. Surman, and A. Bradshaw, Solid State Commun. **57**, 329 (1986).

[27] J. Hermanson, Solid State Commun. **22**, 9 (1977).

[28] J. Callaway and C. S. Wang, Phys. Rev. B **16**, 2095 (1977).

[29] W. F. Egelhoff, Jr., Phys. Rev. B **30**, 1052 (1984).

[30] Chanyong Hwang, A. K. Swan, and S. C. Hong, Phys. Rev. B **60**, 14 429 (1999).

[31] V. L. Moruzzi, P. M. Marcus, K. Schwarz, and P. Mohn, Phys. Rev. B **34**, 1784 (1986).

[32] B. T. Thole, P. Carra, F. Sette, and G. van der Laan, Phys. Rev. Lett. **68**, 1943 (1992).

[33] C. T. Chen, Y. U. Idzerda, H.-J. Lin, N. V. Smith, G. Meigs, E. Chaban, G. H. Ho, E. Pellegrin, and F. Sette, Phys. Rev. Lett. **75**, 152 (1995).